Revista ALCONPAT
www.revistaalconpat.org
eISSN 2007-6835
Revista de la Asociación Latinoamericana de Control de Calidad, Patología y Recuperación de la Construcción

Influence of thermal curing on the physical and mechanical properties of ultra-high-performance cementitious composites with glass powder

F. G. S. Ferreira[1]*, L. V. Dias[1], S. M. Soares[2], A. L. Castro[3]
*Contact author: fgiannotti@ufscar.br
DOI: https://doi.org/10.21041/ra.v12i2.546

Reception: 13/07/2021 | Acceptance: 28/02/2022 | Publication: 01/05/2022

ABSTRACT

This paper discusses the impact of thermal curing and particle packing on ultra-high-performance concrete (UHPC) that used glass powder as a partial replacement of Portland cement. For this, specimens with 0% and 50% of glass powder (volumetric substitution to cement) were produced, as well as two mixtures obtained by particle packing. The samples were submitted to thermal and standard curing to compare the effects and tested for compression strength and capillary water absorption. The results show that thermal curing improves resistance expressively in the early ages while particle packing applied to the mix design improved significantly the concrete properties, indicating that glass powder is a viable substitute for cement.

Keywords: cementitious composite; thermal curing; particle packing; glass powder.

Cite as: Ferreira, F. G. S., Dias, L. V., Soares, S. M., Castro, A. L. (2022), "*Influence of thermal curing on the physical and mechanical properties of ultra-high-performance cementitious composites with glass powder*", Revista ALCONPAT, 12 (2), pp. 184 – 199, DOI: https://doi.org/10.21041/ra.v12i2.546

[1] Departamento de Engenharia Civil, Universidade Federal de São Carlos, São Carlos, Brasil.
[2] Instituto Federal de Educação, Ciência e Tecnologia de São Paulo, Caraguatatuba, Brasil.
[3] Departamento de Engenharia de Estruturas, Universidade de São Paulo, Brasil.

Contribution of each author
In this work, the author L. V. Dias contributed with the activities of conceptualization, development, results and discussion, writing and preparation of the original text (30%); S. M. Soares contributed to the activities of conceptualization, development, results and discussion (30%); F. G. S. Ferreira contributed with conceptualization, supervision, discussion of results, writing and review (20%) and A. L. Castro contributed with conceptualization, supervision, discussion of results, writing and review (20%).

Discussions and subsequent corrections to the publication
Any dispute, including the replies of the authors, will be published in the first issue of 2023 provided that the information is received before the closing of the third issue of 2022.

Revista ALCONPAT, 12 (2), 2022: 184 – 199

Influência da cura térmica nas propriedades física e mecânica de compósitos cimentícios de ultra alto desempenho com pó de vidro

RESUMO

Este trabalho visa avaliar o impacto da cura térmica e do uso de empacotamento de partículas em compósitos cimentícios de ultra alto desempenho (CCUAD), com e sem pó de vidro. Para tanto, foram moldados corpos de prova com 0% e 50% de pó de vidro (substituição volumétrica ao cimento), além de dois traços obtidos através do empacotamento de partículas. As amostras foram submetidas a cura térmica e a cura úmida para comparação dos efeitos. Foram realizados ensaios de resistência à compressão e de absorção de água por capilaridade. Os resultados indicaram que a cura térmica proporciona ganho inicial de resistência, a aplicação do empacotamento de partículas na dosagem das misturas resultou em uma significativa melhoria nas propriedades das amostras e o pó de vidro se mostrou um substituto viável para o cimento.

Palavras-chave: compositos cimentícios; cura térmica; empacotamento de particulas; pó de vidro

Influencia del curado térmico en las propiedades físicas y mecánicas del hormigón de ultra alto desempeño con polvo de vidrio

RESUMEN

Este trabajo tiene como objetivo evaluar el impacto del curado térmico y el uso de empaquetamiento de partículas en compuestos cementosos de ultra alto desempeño (UHPC), con y sin polvo de vidrio. Para ello, los cuerpos de prueba fueron moldeados con 0% y 50% de polvo de vidrio (reemplazo volumétrico al cemento), además de dos mezclas obtenidas a través del empaquetamiento de partículas. Las muestras fueron sometidas a curado térmico y curado húmedo para comparar los efectos. Se realizaron pruebas de resistencia a la compresión y absorción por capilaridad. Los resultados indicaron que el curado térmico proporciona ganancia de la resistencia inicial, la aplicación del empaquetamiento de partículas en las dosis de mezcla resultó en una mejora significativa en las propiedades de las muestras y el polvo de vidrio demostró ser un sustituto viable del cemento.

Palabras chave: compuestos cementosos; curado térmico; empaquetamiento de partículas; polvo de vidrio

1. INTRODUCTION

In the last decades, ultra-high-performance cementitious composites (UHPCC) emerged to meet the growing demand for more durable structures with higher mechanical resistance. The first reference to the term is attributed to de Larrard and Sedran, in 1994 (Shi *et al.*, 2015), while referring to a composite with high mechanical resistance (greater than 150 MPa) and high durability (Alkaysi *et al.*, 2016; Wang *et al.*, 2019). To achieve these characteristics, a high cement consumption (about 1000 kg/m³) and a low water/cement ratio (w/c) (between 0.14 and 0.20) are required to allow reduced porosity, and the use of a superplasticizer additive to provide adequate workability to the material (Ganesh and Murthy, 2019). The inclusion of silica fume also changes workability while increasing the final strength due to the better filling of the voids and the generated pozzolanic reactions (Abbas *et al.*, 2015).

The application of particle packing models is necessary to determine the composition of special mixtures, such as UHPCC, since they improve the mechanical properties and the durability of the cementitious composite, by increasing the matrix density (Castro and Ferreira, 2016). The packing concept also contributes to increasing density with the removal of coarse aggregate (Zhang *et al.*, 2019). Additionally, by removing the coarse aggregate, the internal voids and the transition zone are reduced while generating a more homogeneous distribution of tensions in the grains (Tutikian *et al.*, 2011).

The first published references on particle packing date back to 1892 and are attributed to Féret (Castro and Pandolfelli, 2009). In 1930, Furnas developed one of the first packing models, based on a discrete approach. Subsequently, a model based on continuous distributions was developed by Andreasen. Finally, Funk and Dinger (1994) analyzed both models and reported that the models proposed approximately the same solution. Therefore, the authors perfected their model that became known as Alfred's model, whose analysis is considered to generate the best results (Lopes, 2019).

The adopted curing procedure also influences the development of mechanical resistance in cementitious composites such as UHPCC. Thermal curing procedures at temperatures between 90 and 400 °C, can maximize the composite mechanical strength due to the acceleration of pozzolanic reactions, improving the matrix microstructure (Ganesh and Murthy, 2019).

The main effect of thermal curing in concretes is linked with the increase in density generated by the greater amount of C-S-H produced (Bahedh and Jaafar, 2018). Such a process, when performed in a high humidity environment at 90 °C, increases significantly the concrete strength in the early ages (Heinz *et al.,* 2012). However, Terzian (2005) asserted that thermal curing procedures performed at temperatures above 70 °C can reduce concrete final strength between 10 and 20%.

The incorporation of mineral additions can provide a better particles packing and also contribute to the reduction of the environmental impact. The environmental impact of the cement manufacturing process is enormous since 0.8 tons of CO_2 is released to produce one ton of cement (Mehta and Ashish, 2020). To this end, the high consumption of cement required for producing UHPCC has an extremely significant environmental impact. Therefore, looking for a viable replacement for cement that does not modify significantly the composite properties is interesting and desired. The glass powder characteristics allow its use as a possible substitute for cement due to the significant pozzolanic activity resulting from the high content of silica (SiO_2) and its amorphous structure, in addition to being abundant. In 2005, the USA generated 12.8 million tons of waste, of which only 2.75 million were recycled (Schwarz *et al.*, 2008) and, in 2007, the European Union generated about 25.8 Mt of glass waste (Abdollahnejad *et al.*, 2017). Furthermore, in 2008, Brazil consumed 5.5 kg of glass packaging per inhabitant, of which 80% have not been recycled (IPEA, 2012).

The main objective of this work is to evaluate the effects of thermal curing on UHPCC specimens

Revista ALCONPAT, 12 (2), 2022: 184 – 199

with and without added glass powder.

2. PROCEDURE

2.1 Materials

This research used as binders Portland cement of high initial resistance (CPV ARI), silica fume, and glass powder consisting of ground recycled amber bottles that were subsequently sieved in the #200 mesh sieve (diameter less than 75 μm). Also, natural quartz sand was used as fine aggregate. Additionally, ground silica (SM200) was used as filler, the superplasticizer additive based on polycarboxylate provided adequate workability due to the low water/binder ratio used, and shrinkage reducing additive to avoid cracking of the matrix. The parameters of the granular materials used to produce the UHPCC are shown in Tables 1 to 4.

Table 1. Portland Cement physical characteristics.

Parameter		Method	Obtained value	Reference value, NBR 16697 (ABNT, 2018)
Specific gravity		NBR 16605 (ABNT, 2017)	3.16 g/cm³	-
Initial setting time		NBR 16607 (ABNT, 2018)	135 min	≥ 60 min
Final setting time		NBR 16607 (ABNT, 2018)	210 min	≤ 600 min
Water for normal consistency		NBR 16606 (ABNT, 2018)	30.0%	-
% retained in 75 μm sieve		NBR 16372 (ABNT, 2015)	0.1%	≤ 6.0%
Blaine surface area		NBR 16372 (ABNT, 2015)	665.0 m²/kg	-
Compressive strength	1 day	NBR 7215 (ABNT, 2019)	27.5 MPa	≥ 14.0 MPa
	3 days		42.0 MPa	≥ 20.0 MPa
	7 days		48.7 MPa	≥ 34.0 MPa
	28 days		52.2 MPa	-

Table 2. Silica fume, glass powder and filler physical characteristics.

Parameter	Silica fume		Glass powder		Filler	
	Test results	Reference value NBR 13956-1	Test results	Reference value	Test results	Reference value
Specific gravity	2.25 g/cm³	-	2.55 g/cm³	-	2.70 g/cm³	-
Moisture		≤ 3.0%	-	-	-	-
% retained in 45 µm sieve	Max. 10.0%	≤ 10.0%	-	-	-	-
Blaine surface area	247.0 m²/kg	-	393.0 m²/kg	-	234.0 m²/kg	-
Pozzolanic activity index	Min. 105.0%	≥ 105.0%	6.4 MPa	6.0 MPa**	-	-

*tested according to the NBR 5751 (ABNT, 2015) method.
** Reference values from NBR 12653 (ABNT, 2015).

Table 3. Materials chemical composition.

Component	Materials (% mass)			
	Portland cement	Silica fume	Glass powder	Fine aggregate
Loss on ignition (LOI)	4.05 (≤ 6,50)*	3.60(≤ 6,00)**	0.58	0.58
Calcium oxide (CaO)	61.40	<0.20	9.10	0.071
Aluminum oxide (Al_2O_3)	4.31	<0.20	3.70	3.40
Silicic anhydrous (SiO_2)	23.00	94.10	74.00	94.00
Sulfur trioxide (SO_3)	2.97 (≤4,5)*	-	-	-
Ferric oxide (Fe_2O_3)	2.49	<0.50	0.42	0.67
Potassium oxide (K_2O)	0.96	1.28	0.56	1.20
Phosphoric oxide (P_2O_5)	0.52	-	-	-
Strontium oxide (SrO)	0.27	<0.20	0.039	-
Chlorine ions (Cl^-)	0.12	-	-	-
Thorium dioxide (ThO_2)	<0.01	<0.01	<0.01	<0.01
Uraninite (U_3O_8)	<0.01	<0.01	<0.01	<0.01
Titanium dioxide (TiO_2)	-	<0.20	-	0.35
Chromium oxide (Cr_2O_3)	-	-	-	0.049
Magnesium oxide (MgO)	-	-	0.74	-
Rubidium oxide (Rb_2O)	-	-	0.016	-
Sodium oxide (Na_2O)	-	-	11.00	0.37

* Reference values of NBR 16697 (ABNT, 2018).
** Reference values of NBR 13956-1 (ABNT, 2012).

Revista ALCONPAT, 12 (2), 2022: 184 – 199

Table 4. Fine aggregate physical characteristics.

Parameters	Method	Obtained value
Water absorption	NBR 16916 (ABNT, 2021)	0.64%
Specific gravity	NBR 16916 (ABNT, 2021)	2.56 g/cm³
Unit weigth	NBR 16972 (ABNT, 2021)	1475.78 kg/m³
Unit weigth (compacted)	NBR 16972 (ABNT, 2021)	1617.83 kg/m³
Organic impurities	NBR NM 49 (ABNT, 2006)	Clear solution than standard
Fine material passing through the 75 µm sieve, by washing	NBR 16973 (ABNT, 2021)	1.66%

Figure 1 shows the particle size distribution of cement, silica fume, glass powder, fine aggregate (quartz sand), and filler (SM200). The d50 values of 0.8, 7, 15, 32, and 270 µm were determined for silica fume, cement, glass powder, filler, and fine aggregate, respectively.

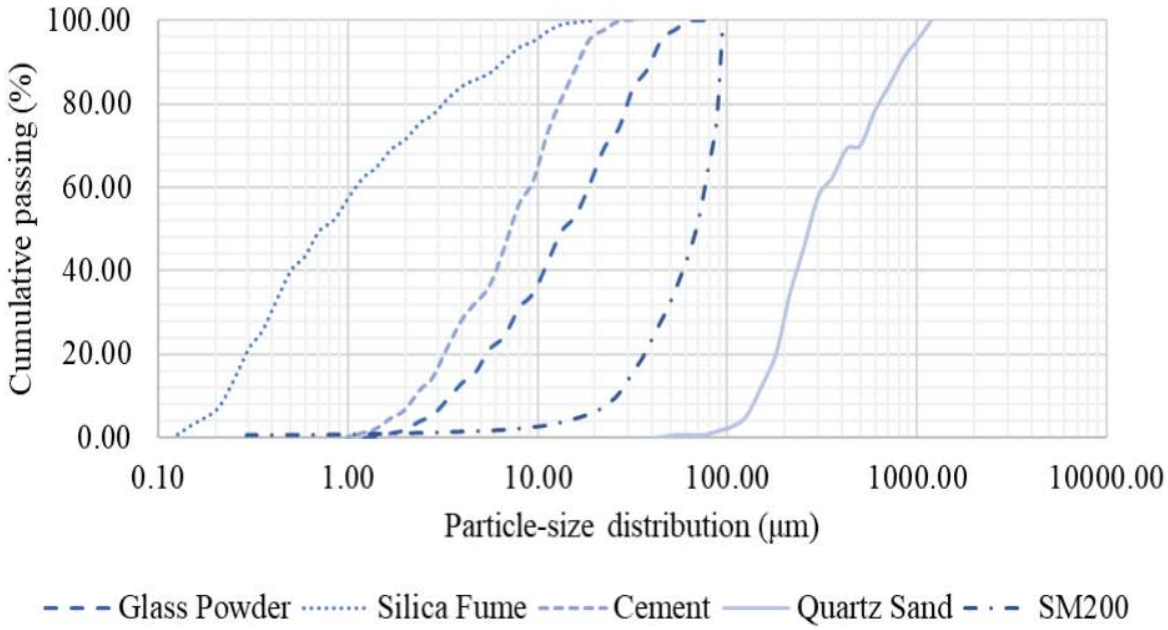

Figure 1. Particle size distribution of granular materials in the UHPCC.

2.2 Methodology

To produce all UHPCC mixtures, a fixed water/binder ratio of 0.18 was adopted. Initially, two mixtures were produced, a reference mix (REF), with 0% added glass powder, and a mix with 50% glass powder (GP50) as a volumetric replacement for cement; silica fume was added to both mixtures, at a ratio of 8% to the cement mass of the reference mix. Subsequently, the GP50 mix was optimized based on the particle packing concept, applying the Alfred model (Equation 1).

$$CPFT = \left(\frac{D_p^q - D_S^q}{D_L^q - D_S^q}\right) \times 100 \quad (1)$$

Where: CPFT is the cumulative percent finer than D_p, D_p is the particle diameter, D_L is the largest particle diameter in the size distribution, D_S is the smallest particle diameter in the size distribution, and q is a constant, designated per particle size distribution module.

The distribution coefficient value used for optimizing the GP50 mix was determined considering the discrete particle size distribution and the proportions of materials added in the mixtures. Thus, the experimental curve was obtained for the particle size distribution while the theoretical curve was obtained by applying the Alfred model. Through an iterative process to adjust the theoretical curve to the experimental curve, aiming to obtain the maximum correlation coefficient, the distribution coefficient value was determined ($q = 0.17$; $R^2 = 0.9913$).

The mixture composition was optimized by a mathematical process, which used as input data the discrete particle size distribution of the materials added to the mixture and the distribution coefficient determined for the GP50. Iteratively, the program calculates the diameter of the smallest and largest particles present in the mixture, providing the theoretical grain size distribution curve of the adopted packing model (Alfred model). Simultaneously, the content of each added material is adjusted to obtain the highest correlation coefficient between the theoretical and experimental curves. At the end of the process, the optimized mixture composition is given in terms of the mass percentage of each granular material added to the mixture.

Thus, a spreadsheet editor, using the solver tool, assisted the calculations of the optimal proportion of the materials constituting the optimized mixture, identified as GP50E. Figure 2 shows that the particle size range between the sand and the glass powder is not filled by any particle of the granular materials added initially. For this reason, to increase the packing efficiency of the selected mixture, the filler (SM200) was added to the list of materials that make up the mixture (Figure 3), generating a second optimized mixture based on the particle packing concept (GP50SM), applying the Alfred model and the determined distribution coefficient value.

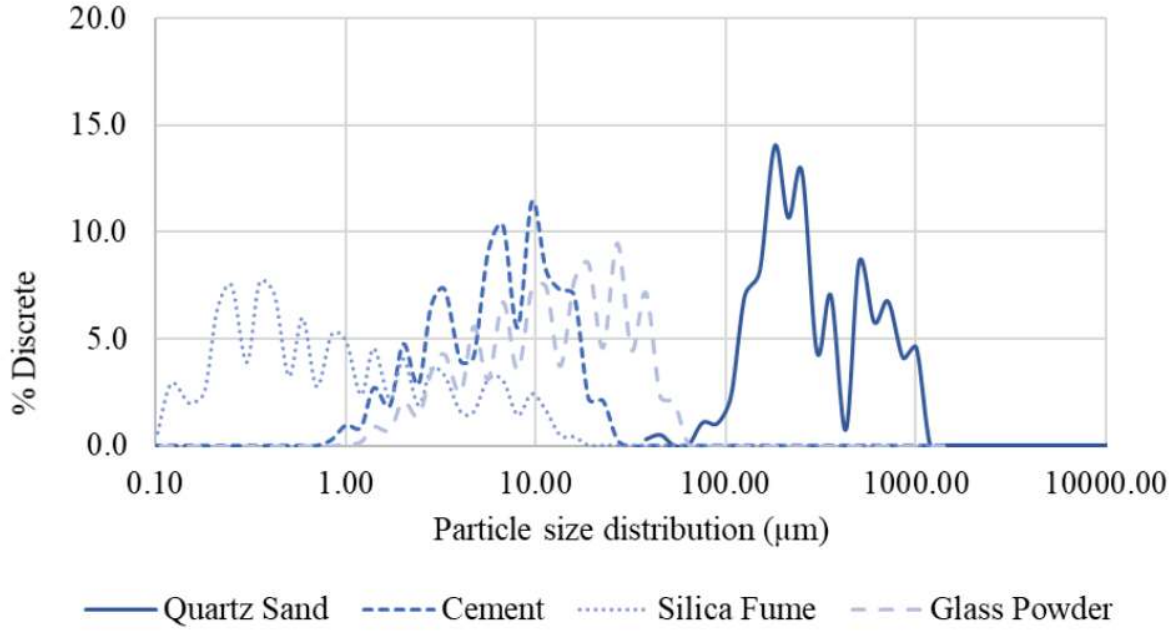

Figure 2. Discrete particle size distribution of materials without SM200.

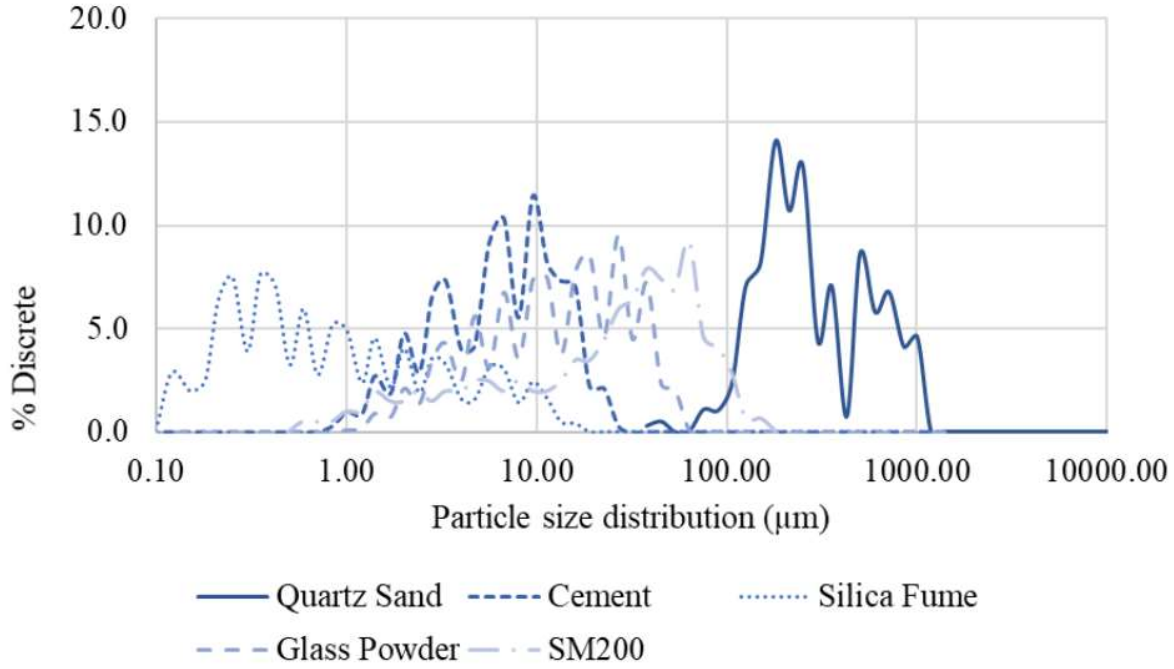

Figure 3. Discrete particle size distribution of materials with SM200.

Table 5 shows the unitary mix cementitious composites (in mass), the consistency index, and the cement consumption for the studied mixtures. Consistency was measured according to NBR 13276 (ABNT, 2016). It is noteworthy that the content of the superplasticizer additive was determined to obtain a consistency of (380 ± 10) mm (fluid consistency) for the REF and GP50 mixtures, maintaining the same superplasticizer content when producing the optimized mixtures to reduce the variables in the process. The shrinkage-reducing additive content was determined following the manufacturer's recommendations. The compatibility between the binders and the additives was verified through the mini-slump test (Kantro, 1980).

Table 5. Mixtures proportion, consistency index and cement consumption of UHPCC.

Mixtures	Cement	Silica fume	Glass powder	Fine aggregate	Filler	Water	SP*	RR**	Consistence index (mm)	Cement consumption (kg/m³)
REF	1	0.08	0	1.07	0	0.18	0.02	0.01	380	1,000
GP50	1	0.16	0.81	2.15	0	0.18	0.04	0.02	385	500
GP50E	1	0.43	0.46	2.11	0	0.18	0.04	0.02	345	510
GP50SM	1	0.29	0.40	2.01	0.30	0.18	0.04	0.02	323	514

*Superplasticized additive.
**Shrinkage reducing additive.

Then, cylindrical specimens of 50 mm x 100 mm were manually molded, following a material mixing procedure developed during the research and suitable for each different mix (Figure 4). When producing the GP50SM mix, the glass powder and filler were weighed separately, packed in the same package, and homogenized for about 2 minutes before being added to the mixture.

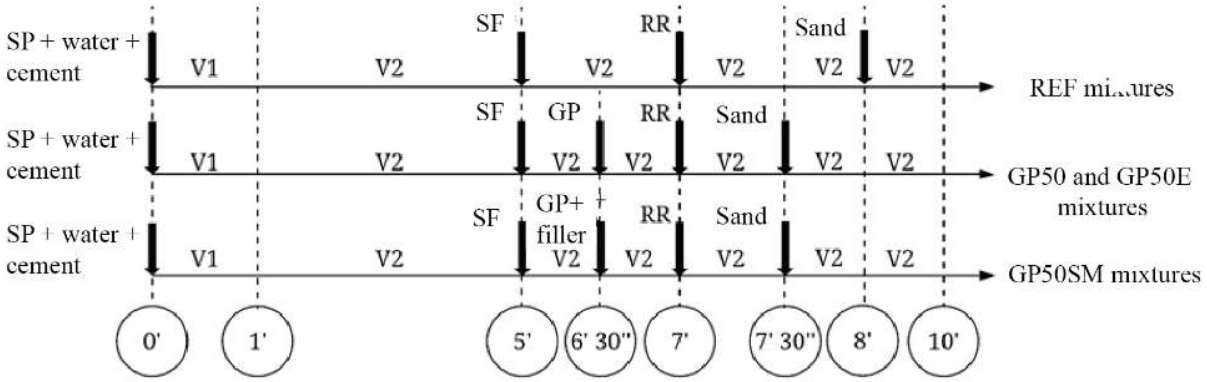

Figure 4. The mixing procedure, in which V1 and V2 represent, respectively, the low and high speeds of the mortar mixer/pump/machine.

After molding, the specimens were placed in an air-conditioned chamber for approximately 48 hours, until demolding. The specimens were then submitted to the respective curing procedures. For thermal curing (TC), the specimens were placed in an appropriate container/tank filled with water, ensuring that all were fully submerged. This container was placed in an unventilated oven heated to (90 ± 5) °C for two hours, corresponding to a heating rate of approximately 35 °C/h. After 24 hours in the oven, all specimens were removed and taken to an air-conditioned room, where they remained for 24 hours. Finally, the specimens were placed in a container filled with lime-saturated water until the testing ages. Another group of specimens was submitted to immersion curing (IC), which consists of immersion in lime-saturated water.

Then, the mechanical resistance of the specimens was determined at the ages of 7, 28, and 180 days, for a total of 8 specimens per mixture (4 for TC and 4 for IC) using the axial compression test, according to NBR 5739 (ABNT, 2018). Additionally, capillary water absorption was evaluated at 28 days of age, for 6 specimens per mix (3 for TC and 3 for IC), according to NBR 9779 (ABNT, 2012). The obtained results were analyzed using Analysis of Variance (ANOVA) and F> Critical indicated significant statistical differences in the group, the means were compared by Tukey test to verify which sample was significantly different.

3. RESULTS AND DISCUSSIONS

3.1 Compressive strength

Figure 5 shows graphically the compressive strength results for the studied mixtures. The values are the average of four individual values obtained from the specimens tested at the ages of 7, 28, and 180 days.

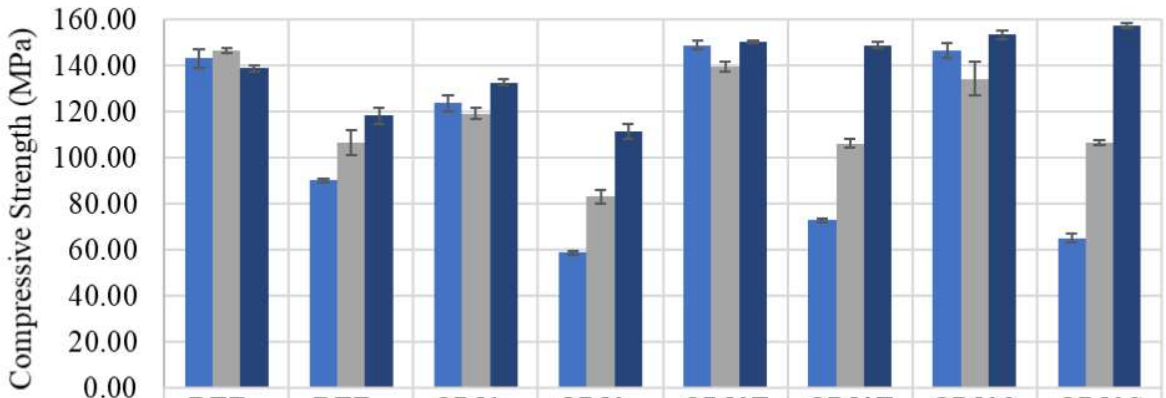

	REF - TC	REF - IC	GP50 - TC	GP50 - IC	GP50E - TC	GP50E - IC	GP50SM - TC	GP50SM - IC
7 days	143.16	90.10	123.62	58.81	149.01	72.81	146.51	65.19
28 days	146.64	106.37	119.15	83.06	139.59	106.22	134.26	106.65
180 days	138.85	118.31	132.78	111.58	150.51	148.98	153.39	157.38

Figure 5. Compressive strength of the UHPCC mixtures.

At 7 days of age, the comparison of different cure types shows that the resistance values are about 2 times higher for specimens submitted to TC compared to IC, except for the REF mix, whose resistance is about 1.6 times higher. This resistance gain can be attributed mainly to the acceleration of the cement hydration reactions and the pozzolanic reactions of the added minerals, and the exposure to a temperature of (90 ± 5) °C during the thermal curing process. However, at 180 days, this gain is not so significant since the TC/IC ratio varied between 0.97 and 1.17. This result can be explained by the fact that the thermal cure only accelerates the process to reach the composite final strength, thus having little impact on the resistance in later ages, especially in mixtures optimized through the packing of particles. Likewise, other authors evaluated the performance of UHPCC mixtures under different curing conditions and observed similar behavior. Heinz *et al.* (2012) compared the mechanical performance of UHPCC using cubic specimens submitted to thermal and immersion curing and reported that resistance values of 136.3 MPa (IC) increased to 232.5 MPa (TC) at 7 days of age (1.76 times greater) whereas, at 28 days, resistances of 216.1 MPa (IC) increased to 232.8 MPa (TC) (1.08 times greater). Sokolovicz (2020) investigated the behavior of UHPCC specimens obtained by packing particles and reported resistances 1.25 times greater at 7 days and 1.13 at 28 days, to those submitted to thermal curing compared to immersion curing.

Additionally, the loss of resistance in specimens submitted to TC, between 7 and 28 days (Fig. 5), is not significant according to the ANOVA statistical analysis and the Tukey test. Melo (2000) attributed this resistance loss to the changes in concrete microstructure caused by the accelerated process of cement hydration, but resistance improves again due to the pozzolanic activity of silica fume at more advanced ages (180 days). Additionally, Du and Tam (2015) verified that the pozzolanic reactions of the glass powder are slower compared to the cement hydration process, which may have also contributed to the later recovery of the resistance of the specimens with added fine material.

Initially, the samples optimized via particle packing had no significant resistance gain compared to traditionally dosed mixtures. At 7 days of age, the resistance of the GP50E and GP50SM specimens is lower than the reference but statistically equal to the resistance of the GP50 mix. This fact can be explained by the lower cement consumption of the GP50, GP50E and GP50SM mixtures compared to the REF mixture, which probably impaired the mechanical performance of these mixtures in the early ages. At more advanced ages, a significant compressive strength gain is

observed for the optimized samples. Lopes (2019) also investigated concrete optimized via particle packing and observed significant strength gains after 28 days of age, attributing them to the strengthening transition zones due to mineral additions. Similarly, this justification can also be applied to this case since the optimized mixtures consumed high amounts of silica fume. Sokolovicz (2020) evaluated the mechanical behavior of UHPCC packaged, submitted to wet curing, and reported resistances of 115.30, 138.60 and 158.9 MPa, at 7, 28 and 91 days, respectively. In this case, resistance developed more uniformly over time, probably explained by the fact that the specimens consumed less silica fume and the non-use of glass powder, which has slower pozzolanic activity, as previously mentioned. It is also observed that the author reported a final resistance close to that obtained in the present study.

It is noteworthy that the development of compressive strength of the studied UHPCC occurs as a function of cement hydration and the pozzolanic reaction of silica fume and glass powder. Depending on the type and content of mineral addition used and the curing regime adopted, a significant gain in strength can occur at ages greater than 28 days (as can be seen in Figure 5 for compressive strength at 180 days), a fact that must be considered in the design of concrete structures.

3.2 Water absorption

Figure 6 shows graphically the results of the capillary water absorption test obtained for the studied mixtures. The values are the average of three individual measurements obtained from the specimens tested at 28 days.

	REF - TC	REF - IC	GP50 - TC	GP50 - IC	GP50E - TC	GP50E - IC	GP50SM - TC	GP50SM - IC
28 days	0.360	0.793	0.914	0.882	0.544	0.552	0.335	0.384

Figure 6. Capillary water absorption of the studied UHPCC mixtures.

Figure 6 shows that the lowest levels of water absorption by capillarity were recorded for the specimens optimized via particle packing, considering the use of SM200 (GP50SM). This result can be explained by the filler effect provided by the material, which provides a more dense and homogeneous microstructure while generating a disconnected pore structure and reducing the water absorption by the material (Tam *et al*., 2012). Also, the optimized samples (GP50E and GP50SM), in general, absorbed less water than those traditionally dosed, which can be explained by the better filling of the voids provided by the particle packing and by the high consumption of silica fume which, in addition to the filler effect, provides an additional amount of CSH due to the pozzolanic reaction, blocking the pores present in the material (Tam *et al*., 2012). This effecty also explains why, in general, the samples submitted to TC show less absorption than those submitted

to IC, since this curing procedure increases the C-S-H amount in the early ages due to the acceleration of cement hydration reactions.

It is worth mentioning the great dispersion of results observed for some studied UHPCC, as is the case of the REF-IC and GP50-IC. As the capillary water absorption values obtained for these mixtures are very low (0.793 kg/m^2 for REF-IC and 0.882 kg/m^2 for GP50-IC), a small difference between the values obtained for the specimens can result in a high standard deviation, as observed in the present study, corresponding to coefficients of variation of 10.4% and 26.0%, respectively.

It is noteworthy, however, that the test procedure in NBR 9779 (ABNT, 2012) was not suitable to be applied to UHPCC, since due to the low amount of pores present in the concrete microstructure, the specimens did not present significant mass differences after long periods in the oven or exposed to water.

3.3 Statistical analysis

Tables 6 to 9, presented below, show the statistical analysis results of the mechanical resistance and capillary water absorption of the studied UHPCC mixtures. Yes indicates a statistically significant difference between samples whereas No indicates no statistically significant difference between samples.

Table 6. Mechanical resistance at 7 days - significant difference (F = 68.87 and $F_{obtained}$ = 2.42).

	REF - IC	GP50 - TC	GP50 - IC	GP50E - TC	GP50E - IC	GP50SM - TC	GP50SM - IC
REF - TC	Yes	No	Yes	No	Yes	No	Yes
REF - IC		Yes	Yes	Yes	No	Yes	Yes
GP50 - TC			Yes	Yes	Yes	Yes	Yes
GP50 - IC				Yes	No	Yes	No
GP50E - TC					Yes	No	Yes
GP50E - IC						Yes	No
GP50SM - TC							Yes

According to Table 6, it is possible to observe that there was a significant difference in the values of compressive strength (at 7 days of age) of the samples submitted to TC, compared to the samples after IC. The incorporation of glass powder provided a significant decrease in the mechanical strength of the UHPCC.

Table 7. Mechanical resistance at 28 days - significant difference (F = 9.07 and $F_{obtained}$ = 2.42).

	REF - IC	GP50 - TC	GP50 - IC	GP50E - TC	GP50E - IC	GP50SM - TC	GP50SM - IC
REF - TC	Yes	No	Yes	No	Yes	No	Yes
REF - IC		No	No	Yes	No	No	No
GP50 - TC			Yes	No	No	No	No
GP50 - IC				Yes	No	Yes	No
GP50E - TC					Yes	No	No
GP50E - IC						No	No
GP50SM - TC							No

At 28 days of age (Table 7), it is possible to observe that the mixtures GP50-TC, GP50SM-TC and GP50SM-IC did not present significant differences in relation to most of the studied UHPCC. For the GP50SM mixture, with the incorporation of silica fume, glass powder and filler, the curing procedure (TC or IC) did not imply significant differences in terms of mechanical resistance. The samples with glass powder incorporation ans submitted to TC showed no significant differences compared to the reference sample after TC (REF-TC).

Table 8. Mechanical resistance at 180 days - significant difference (F = 19.84 and $F_{obtained}$ = 2.42).

	REF - IC	GP50 - TC	GP50 - IC	GP50E - TC	GP50E - IC	GP50SM - TC	GP50SM - IC
REF - TC	Yes	No	Yes	No	No	No	Yes
REF - IC		No	No	Yes	Yes	Yes	Yes
GP50 - TC			Yes	No	No	Yes	Yes
GP50 - IC				Yes	Yes	Yes	Yes
GP50E - TC					No	No	No
GP50E - IC						No	No
GP50SM - TC							No

According to Table 8, it is possible to observe that there was a significant difference in the values of compressive strength (at 180 days of age) of the samples submitted to TC, compared to the samples after IC in the REF and GP50 mixtures. In the others, the curing procedure did not significantly interfere with resistance. In the samples submitted to TC, the incorporation of glass powder did not provide a significant difference in the compressive strength of the UHPCC.

Table 9. Water absorption at 28 days - significant difference.

	REF - IC	GP50 - TC	GP50 - IC	GP50E - TC	GP50E - IC	GP50SM - TC	GP50SM - IC
REF - TC	Yes	Yes	Yes	No	No	No	No
REF - IC		No	No	Yes	Yes	Yes	Yes
GP50 - TC			No	Yes	Yes	Yes	Yes
GP50 - IC				Yes	Yes	Yes	Yes
GP50E - TC					No	No	No
GP50E - IC						No	No
GP50SM - TC							No

According to Table 9, it is possible to observe that there was no significant difference in the water absorption values of the samples submitted to TC, compared to the samples after IC, except for the sample without glass powder (REF). The incorporation of glass powder did not provide a significant difference in the water absorption of the UHPCC submitted to TC (except for the GP50 mixture). As for the mixtures with better particle packing (GP50E and GP50SM), the decrease in the values of capillary water absorption was significant, when compared to the GP50 mixture, regardless of the curing procedure.

4. CONCLUSIONS

Given the obtained data, it can be concluded that:

1. The adopted thermal curing procedure is feasible and beneficial since concrete strength increased in early and more advanced ages, especially if applied to cementitious composites with added glass powder.
2. The particle packing model used to optimize the mixtures increased the concrete strength and reduced water absorption effectively; these effects became more pronounced at more advanced ages.
3. The use of ground silica (SM200) did not generate significant strength gains. However, the observed reduction of water absorption validates its use.
4. The high levels of glass powder (50%) added tend to decrease the mechanical strength of the UHPCC by 35%, 22% and 5% compared to the reference composite at 7, 28 and 180 days, respectively, indicating the feasibility of using glass powder as a partial substitute for cement.
5. The water absorption test following the method recommended in the NBR 9779 (ABNT, 2012) is not ideal for evaluating the performance of the UHPCC mixtures. Therefore, it is recommended to elaborate another procedure more appropriate for low porosity and/or permeability composites.

5. ACKNOWLEDGMENTS

To the National Council for Scientific and Technological Development (CNPq) for the financial support to this research and to the Institute of Technological Research of the State of São Paulo (IPT), for assisting the characterization tests of the binders.

6. REFERENCES

Abbas, S., Soliman, A. M., Nehdi, M. L. (2015), *Exploring mechanical and durability properties of ultra-high-performance concrete incorporating various steel fiber lengths and dosages.* Construction and Building Materials. 75: 429–441. https://doi.org/10.1016/j.conbuildmat.2014.11.017

Abdollahnejad, Z., Kheradmand, M., Pacheco-Torgal, F. (2017), *Short-Term Compressive Strength of Fly Ash and Waste Glass Alkali-Activated Cement-Based Binder Mortars with Two Biopolymers.* Journal of Materials in Civil Engineering. 29(7). https://doi.org/10.1061/(ASCE)MT.1943-5533.0001920

Alkaysi, M., El-Tawil, S., Liu, Z., Hansen, W. (2016), *Effects of silica powder and cement type on durability of ultra-high-performance concrete (UHPC).* Cement and Concrete Composites. 66: 47-56. https://doi.org/10.1016/j.cemconcomp.2015.11.005

Associação Brasileira de Normas Técnicas. (2018). *NBR 5739: Concreto – Ensaio de compressão de corpos de prova cilíndricos*. Rio de Janeiro.

Associação Brasileira de Normas Técnicas. (2015). *NBR 5751 Materiais pozolânicos – Determinação da atividade pozolânica com cal aos sete dias*. Rio de Janeiro.

Associação Brasileira de Normas Técnicas. (2019). *NBR 7215: Cimento Portland - Determinação da resistência à compressão de corpos de prova cilíndricos*. Rio de Janeiro.

Associação Brasileira de Normas Técnicas. (2012). *NBR 9779: Argamassa e concretos endurecidos - Determinação da absorção de água por capilaridade*. Rio de Janeiro.

Associação Brasileira de Normas Técnicas. (2013). *NBR 11579: Cimento Portland - Determinação do índice de finura por meio da peneira 75 μm (nº200)*. Rio de Janeiro.

Associação Brasileira de Normas Técnicas. (2016). *NBR 13276: Argamassa para assentamento e revestimento de paredes e tetos – Determinação do índice de consistência*. Rio de Janeiro.
Associação Brasileira de Normas Técnicas. (2012). *NBR 13956-1: Sílica ativa para uso com cimento Portland em concreto, argamassa e pasta. Parte 1: Requisitos*. Rio de Janeiro.
Associação Brasileira de Normas Técnicas. (2010). *NBR 15895: Materiais pozolânicos – Determinação do teor de hidróxido de cálcio fixado – Método Chapelle modificado*. Rio de Janeiro.
Associação Brasileira de Normas Técnicas. (2015). *NBR 16372: Cimento Portland e outros materiais em pó - Determinação da finura pelo método de permeabilidade ao ar (método de Blaine)*. Rio de Janeiro.
Associação Brasileira de Normas Técnicas. (2017). *NBR 16605: Cimento Portland e outros materiais em pó - Determinação da massa específica*. Rio de Janeiro.
Associação Brasileira de Normas Técnicas. (2018). *NBR 16606: Cimento Portland - Determinação da pasta de consistência normal*. Rio de Janeiro.
Associação Brasileira de Normas Técnicas. (2018). *NBR 16607: Cimento Portland - Determinação dos tempos de pega*. Rio de Janeiro.
Associação Brasileira de Normas Técnicas. (2018). *NBR 16697: Cimento Portland - Requisitos*. Rio de Janeiro.
Associação Brasileira de Normas Técnicas. (2021). *NBR 16916: Agregado miúdo - Determinação da densidade e da absorção de água*. Rio de Janeiro.
Associação Brasileira de Normas Técnicas. (2021). *NBR 16972: Agregados - Determinação da massa unitária e do índice de vazios*. Rio de Janeiro.
Associação Brasileira de Normas Técnicas. (2021). *NBR 16973: Agregados - Determinação do material fino que passa pela peneira de 75 μm por lavagem*. Rio de Janeiro.
Associação Brasileira de Normas Técnicas. (2001). *NBR NM 49: Agregado miúdo - Determinação de impurezas orgânicas*. Rio de Janeiro.
Bahedh, M. A., Jaafar, M. S. (2018), *Ultra High-Performance Concrete Utilizing Fly Ash as Cement Replacement under Autoclaving Technique. Case Studies in Construction Materials. 9.* https://doi.org/10.1016/j.cscm.2018.e00202
Castro, A., Ferreira, F. (2016), *Effect of particle packing in the durability of high performance concretes.* RevistaIngeniería de Construcción. 31(2):91 – 104. http://dx.doi.org/10.4067/S0718-50732016000200003
Castro, A. L., Pandolfelli, V. C. (2009), *Revisão: Conceitos de dispersão e empacotamento de partículas para a produção de concretos especiais aplicados na construção civil.* Cerâmica. 55:18-32. https://doi.org/10.1590/S0366-69132009000100003
De Larrard, F., Sedran, T. (1994), *Optimization of ultra-high perfomance concrete by the use of a packing model.* Cement and Concrete Research. 24(6):997-1009. https://doi.org/10.1016/0008-8846(94)90022-1
Melo, A. B. (2020), *"Influência da cura térmica (vapor) sob pressão atmosférica no desenvolvimento da microestrutura dos concretos de cimento Portland"*, Tese (Doutorado), Universidade de São Paulo, p. 296.
Du, H., Tan, K. H. (2014). *Effect of particle size on alkali-silica reaction in recycled glass mortars.* Construction and Building Materials. 66: 275-285. https://doi.org/10.1016/j.conbuildmat.2014.05.092
Funk, J. E.; Dinger, D. R. (1994), *Predictive process control of crowded particulate suspensions: applied to ceramic manufacturing*. New York: Springer Science Business Media.
Ganesh, P., Murthy, A. R. (2019), *Tensile behaviour and durability aspects of sustainable ultra-high performance concrete incorporated with GGBS as cementitious material.* Construction and Building Materials. 197:667-680. https://doi.org/10.1016/j.conbuildmat.2018.11.240
Heinz, D., Urbonas, L., Gerlicher, T. (2012), "*Effect of Heat Treatment Method on the Properties*

of UHPC" in: M. Schimdt, E. Fehling, C. Glotzbach, S. Fröhlich, S. Piotrowski (Eds.), Ultra-High Perfomance Concrete and Nanotechnology in Construction, HiperMat, Kassel, HE, (Germany), pp. 283-290.

Instituto de Pesquisa Econômica Aplicada (IPEA). (2012), "*Diagnóstico dos Resíduos Sólidos Urbanos*". Disponível em: <https://www.ipea.gov.br/portal/images/stories/PDFs/relatoriopesquisa/121009_relatorio_residuos_solidos_urbanos.pdf>. Acesso em: 27 de março de 2020.

Kantro, D. (1980*), Influence of Water-Reducing Admixtures on Properties of Cement Paste—A Miniature Slump Test*. Cement, Concrete and Aggregates. 2(0):95-102. https://doi.org/10.1520/CCA10190J.

Lopes, H. M. T. (2019), *"Aplicação do conceito de empacotamento de partículas na otimização de dosagem de concretos de cimento Portland"*, Dissertação (Mestrado), Universidade de São Paulo, p. 172.

Mehta, A., Ashish, D. K. (2020), *Silica fume and waste glass in cement concrete production: A review*. Journal of Building Engineering. https://doi.org/10.1016/j.jobe.2019.100888

Schwarz, N., Cam, H., Neithalath, N. (2008), *Influence of a fine glass powder on the durability characteristics of concrete and its comparison to fly ash.* Cement & Concrete Composites. 30: 486–496. https://doi.org/10.1016/j.cemconcomp.2008.02.001

Shi, C., Wu, Z., Xiao, J., Wang, D., Huang, Z., Fang. Z. (2015), *A review on ultra-high-performance concrete: Part I. Raw materials and mixture design.* Construction and Building Materials. 101:741-751. https://doi.org/10.1016/j.conbuildmat.2015.10.088

Sokolovicz, B. C. (2020), *"Avaliação das propriedades mecânicas e microestrutura de concreto de ultra alto desempenho com adições minerais e resíduos industriais"*, Tese (Doutorado), Universidade Federal de Santa Maria, p. 358.

Tam, C. M., Tam, V. W. Y., Ng, K. M. (2012). *Assessing drying shrinkage and water permeability of reactive powder concrete produced in Hong Kong.* Construction and Building Materials. 26:79-89. https://doi.org/10.1016/j.conbuildmat.2011.05.006

Terzian, P. (2005), Concreto pré-fabricado. In: Isaia G. C. "Concreto Ensino Pesquisas e Realizações", São Paulo, IBRACON, v.2.

Tutikian B., F., Isaia, G. C., Helene, P. (2011), *Concreto de Alto e Ultra-Alto Desempenho*. In: Isaia, G. C. "Concreto: Ciência e Tecnologia", São Paulo, IBRACON.

Wang, X., Yu, R., Song, Q., Shui, Z., Liu, Z., Wu, S., Hou, D. (2019), *Optimized design of ultra-high-performance concrete (UHPC) with a high wet packing density.* Cement and Concrete Research. 126. https://doi.org/10.1016/j.cemconres.2019.105921

Zhang, H., Ji, T., Lin, X. (2019), *Pullout behavior of steel fibers with different shapes from ultra-high performance concrete (UHPC) prepared with granite powder under different curing conditions.* Construction and Building Materials. 211: 688-702. https://doi.org/10.1016/j.conbuildmat.2019.03.274